

# Forward Scattering Radar for Ground Targets Detection and Recognition

M. Cherniakov, M. Salous, P. Jančovič, R. Abdullah and V. Kostylev  
EE&CE, The University of Birmingham, Edgbaston, Birmingham, B15 2TT

## Abstract

*This paper presents work on the evaluation of a network of Forward Scattering (FS) radar micro sensors for the detection and classification of ground targets. Theory of FS radar systems is described together with practical experiments to evaluate the feasibility of such a system in real-life scenarios, in terms of power budget analysis and resolution.*

Keywords: forward scattering radar, ground target classification, micro-sensors

## Introduction

In this work we present a feasibility study for the use of Forward Scattering Radar (FSR) micro sensors in the detection and classification of ground targets. This work takes previous research [1-5], where the concept and classification methods were developed, a step further. Here, we investigate the use of a network of compact field-deployable FSR sensors as part of a situation awareness system. Such a system is shown in Fig. 1. To this present time, research on such systems has utilised information from acoustic, seismic and other sensors for target detection and classification. The network of FSR sensors presented here can provide additional information an existing system or alternatively, can be deployed as a separate system.

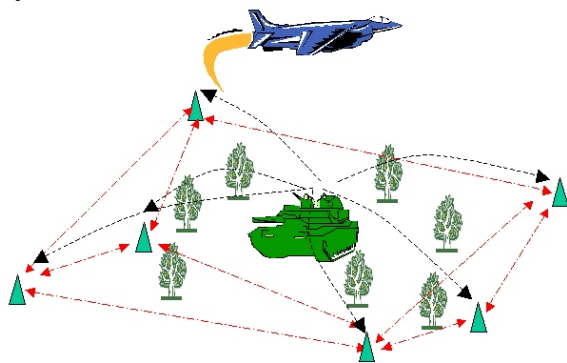


**Fig.1: Micro sensor network for target classification**

In FSR, when a target crosses the baseline between the transmitter and receiver, Doppler recorded by the receiver can then be used to classify targets with reasonably high accuracy. Shadow Inverse SAR algorithms may then be used for classification [6].

Analytic and experimental studies have shown [1-5] that robust classification can be readily achieved. For a single sensor, results have shown that high accuracy can be obtained when vehicles pass the sensor at trajectory angles between  $45^{\circ}$  and  $90^{\circ}$ .

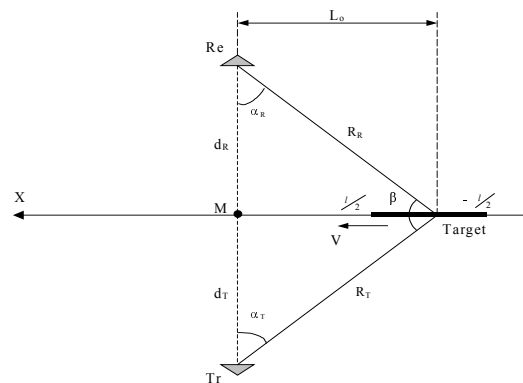


**Fig.2: Forward scattering radar geometry.**

Experiments performed using three sensors clearly show the benefit of a network of sensors, the extra information in yielding better classification performance (Table 1). This is true when assuming both a known and unknown sequence of target trajectory-angles.

**Table 1: Overall classification accuracy using single and multiple observations.**

Angle sequence	Single observation	Three observations
Known	70.4 %	78.4 %
Unknown	53.0 %	70.9 %

### Radar Cross-Section and Power Budget Analysis

Starting from the two-ray model [7], we can describe the power budget of forward scattering radar. Assuming that the surface between the transmitter (Tx) and receiver (Rx) is smooth and perfectly conductive, the received power for vertically polarised antennas is given by (see Fig.2):

$$P_R = P_T G_T G_R \frac{h_T^2 h_R^2}{d^4} \quad (1)$$

where  $P_T$  is the Tx power,  $G_T$  and  $G_R$  are, respectively, the Tx and Rx antenna gains,  $h_T$  and  $h_R$  are, respectively, Tx and Rx elevations and  $d=d_T+d_R$  is the Tx/Rx separation. According to the 2-ray model, power degrades as a function of  $1/d^4$ . In practice, this dependence can be described as:

$$P_R \sim \frac{1}{d^\alpha} \quad (2)$$

where  $\alpha$  is the power term whose value is found experimentally. Although this dependence has been well documented, all known data refers to a non-zero antenna elevation. In our system, the most probable scenario is one in which the antennas are directly on (or near to) the ground. To verify this dependence practically, experiments were conducted on a flat tennis court. Using  $h_T=h_R=0.1$  and  $h_T=h_R=0.75$ m, three antenna types: Horizontal Polarisation (HP), Vertical Polarisation (VP) and Circular Polarisation (CP), were tested. The results are shown in Fig.3.

Table 2 shows the values of  $\alpha$  for tested antenna types and elevations. Although the HP antenna gave the best performance, because of the arbitrary antenna orientation

in the envisaged application, CP may be recommended where technically feasible.

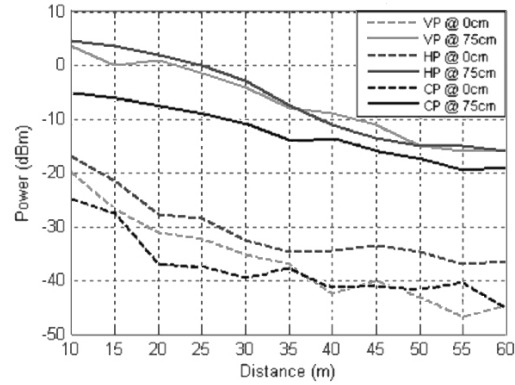


**Fig.3: Received power vs antenna separation.**

**Table 2: The rounded-up values for experimental results for the power term.**

	$h_T = h_R \approx \lambda$
VP	3.5
HP	2.5
CP	3

### Evaluation of RCS Power

The RCS in FSR is known to be:

$$G = \frac{4\pi A^2}{\lambda^2} \quad (3)$$

where  $A$  is the target area and  $\lambda$  is the carrier wavelength. When a ground target is considered, the power density is non-uniformly distributed with elevation and therefore this equation cannot be used. Assuming a rectangular target, that has a width  $l$  and height  $b$ , it can be shown that when placed between the Tx and Rx, the power of the electromagnetic waves at the Rx due to this target, assuming  $\alpha=3$ , is:

$$P_{target} = P_T G_T G_R h_T^2 h_R^2 \frac{4\pi A b^4 B}{10\lambda (d_T d_R)^3} \quad (4)$$

where  $B$  has the units  $m^{-2}$ .  $P_{target}$  is our desired signal as it contains the Doppler shift. From this point onwards, we will assume the following values  $P_T = 10mW$ ,  $G_T$ , and  $G_R = 1$  and that target dimensions (in metres) of  $0.3 \times 1.7$ ,  $6 \times 3$  and  $10 \times 3$  correspond to a human, tank and a truck, respectively.

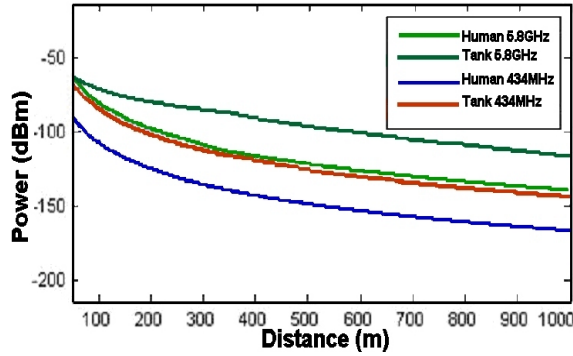


**Fig.4: Power degradation for human and tank, using CP antennas at 0.1m elevation for 434MHz and 5.8GHz.**

Fig.4 illustrates the trend in power signal as a function of antenna separation. It is assumed that  $d_T = d_R$ , corresponding to the minimum received power. It is clear that the larger the target dimensions, especially target height, the larger the resulting signal power. Changing a target's width (the difference, for example, between a truck and a tank) will have a smaller effect compared to changing target height (the difference, for example, between a human and a tank).

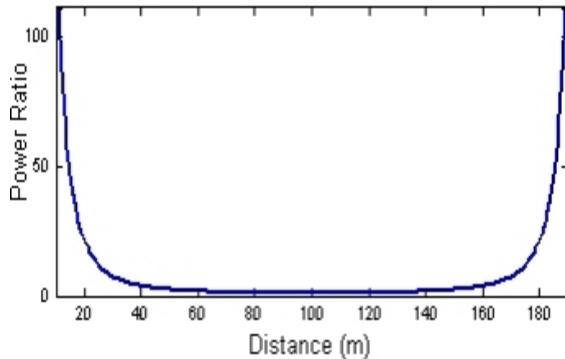


**Fig.5: Blocked power as a function of target placement between the Tx and Rx.**

Fig.5 shows the variation of signal power as the target is placed at different distances between the transmitter and receiver, assuming the distance itself is constant. An important issue to note here is that if a small object is present near either the transmitter or receiver, irrespective of its size, it can result in a significantly high interference level at the receiver.

### Evaluation of Signal to Noise Ratio Due to the Presence of a Screen

To evaluate the Signal-to-Noise Ratio (SNR) at the receiver, we use the following equation:

$$SNR = \frac{P_{target}}{kTN_f\Delta f} \quad (5)$$

where  $P_{target}$  is the signal power,  $k$  is Boltzmann's constant,  $T$  is the temperature,  $N_f$  is the noise figure and  $\Delta f = 1/T_I$  where  $T_I$  is the signal integration time.

For the configuration shown in Fig.6, it can be shown that the maximum integration time corresponds to target visibility and is given by:

$$T_{i\max} = \frac{2d_R\lambda}{V_n l} \quad (6)$$

In Table 3, a number of examples illustrate this for different frequencies using  $d_R=100m$ , with  $V_n=1m/s$  for a human target and  $V_n=5m/s$  for a tank and truck.

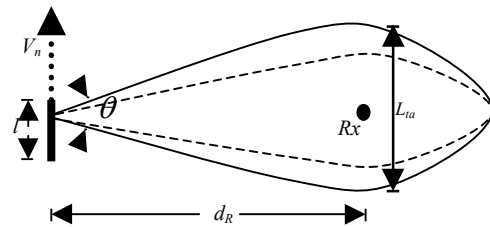


**Fig.6: Scenario to evaluate integration time.**

**Table 3: Theoretical integration times for different targets and frequencies.**

	$f_c=5.8GHz$ $\lambda=0.052m$	$f_c=2.45GHz$ $\lambda=0.12m$	$f_c=890MHz$ $\lambda=0.34m$	$f_c=434MHz$ $\lambda=0.69m$
Human	34.7s	80s	226.7s	460s
Tank	0.34s	0.8	2.26s	4.6s
Truck	0.21s	0.48s	1.36s	2.76s

Using Eqn.6, the maximum SNR is given by:

$$SNR_{i\max} = \frac{4}{V_n kTN_f} \frac{\pi b^5 P_T G_T G_R h_T^2 h_R^2}{5\lambda d_T^3 d_R^2} \quad (7)$$

It is an interesting result that the potentially achievable SNR does not depend at all on

target width, as it is compensated for by the integration time. The graph in Fig.7 shows the SNR as a function of distance between the Tx and Rx, where  $h_T=h_R=0.1$ ,  $d_T=d_R=100\text{m}$ ,  $N_f=10$  and  $T=300$ .

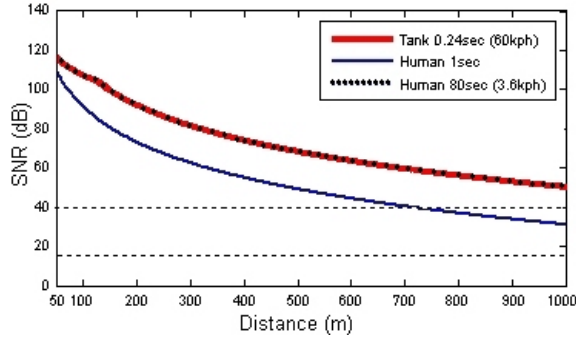


**Fig.7: SNR versus distance for  $f_c=2.45\text{GHz}$ .**

Fig.7 also includes graphs for human targets integrated over 1 second as its reference. Even with the short integration time, both detection (15dB) and classification (40dB) should be possible for up to 600m. In reality, Line of Sight (LOS) reduces this to 100-200m when practical issues such as low antenna elevation and local landscape are taken into consideration.

### FSR Cross-Range Resolution

In this section, we describe the behaviour of the FSR system for the case where a convoy of targets, ranging from tanks to humans on foot, passes through the system. Referring to Fig.2, M is the point where a target crosses the baseline;  $\alpha_T$  and  $\alpha_R$  are the target trajectory angles from the Tx and Rx respectively. For a rectangular target, the received signal is given as:

$$S(t) = \frac{K\lambda}{2\pi vt(d)} \sin\left(\frac{2\pi l}{\lambda} \left(\frac{vt}{d}\right)\right) e^{-j\frac{4\pi}{\lambda}(d)} \quad (8)$$

where K is the coefficient proportional to amplitude of the received signal and  $v$  is the target velocity. Signals representing a human and tank are shown in Fig.8.

Supposing that two closely spaced, similarly sized targets pass through the baseline in sequence, the signal mainlobes may overlap rendering classification more

difficult. Moreover, when a convoy of targets of different sizes passes through the system, the smaller target may be buried within the sidelobes of a larger target.

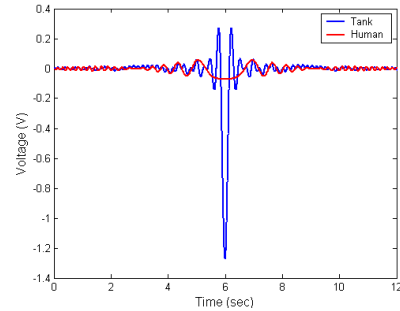


**Fig.8: Plot of signals diffracted by both a human target and a tank.**

### Potential Resolution of Two Equal-Sized Targets

In general, the cross range resolution for SAR is estimated using:

$$\Delta R_c \approx \frac{1}{\Delta f} \quad (9)$$

where  $\Delta R_c$  is a range resolution and  $\Delta f$  is the Doppler bandwidth. Let us consider the simplified scenario, shown in Fig.9.

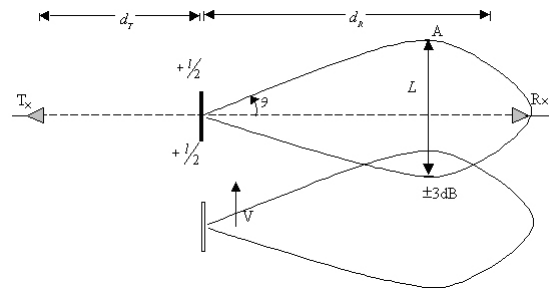


**Fig.9: Rx receiving the main lobe from the first target.**

When the receiver is illuminated by the signal from the main lobe of the target shadow, the target is seen at  $\theta$  angle:

$$\theta = \frac{\lambda}{2l} \quad (10)$$

Therefore, the signal diffracted from a point 'A' has the Doppler shift:

$$f_{d \max} = \frac{2V}{\lambda} \sin \theta \approx \frac{2V}{\lambda} \theta = \frac{V}{l} \quad (11)$$

The path  $L$ , corresponding to the target shadow length at the point of the receiver is given by:

$$L = 2\theta d_R = \frac{\lambda}{l} d_R \quad (12)$$

Alternatively, the target visibility time (at – 3dB level) is given as:

$$T_o = \frac{L}{V} = \frac{2\theta d_R}{V} = \frac{2d_R}{V} \cdot \frac{\lambda}{2l} = \frac{\lambda d_R}{lV} \quad (13)$$

The pulse compression ratio is known to be:

$$P_K = BT \quad (14)$$

where  $B$  is the signal bandwidth and  $T$  is its duration. In our case, the signal has an amplitude modulation that follows the main lobe of duration  $T_o$  of the shadow pattern, i.e.  $\sin(x)/x$  (Fig.10(a)). The signal bandwidth ranges from  $+f_{dmax}$  to  $-f_{dmax}$ , hence:

$$P_K = BT = \frac{\lambda d_R}{l^2} \quad (15)$$

At the correlator output the signal will have a duration of:

$$T_{com} = \frac{T_o}{P_K} = \frac{\lambda d_R l^2}{lV \lambda d_R} = \frac{l}{V} \quad (16)$$

The cross-resolution is:

$$\Delta R_c = VT_{com} = \frac{Vl}{V} = l \quad (17)$$

This equation fits well with the general SAR resolution theory, where the potential  $\Delta R_c$  does not depend on Tx/Rx separation. In our case, the target acts as a secondary antenna.

The graph of Fig.10(b) shows the signal at the output of the correlator where the linear resolution corresponds to about 0.3 – 0.4m, which is equal to the target's length. In order to provide an  $\Delta R_c$ , the signal should be processed using a matched filter:

$$S_{out}(\tau) = \int_{-\infty}^{\infty} S_{in}(t) \cdot S^*(t - \tau) dt \quad (18)$$

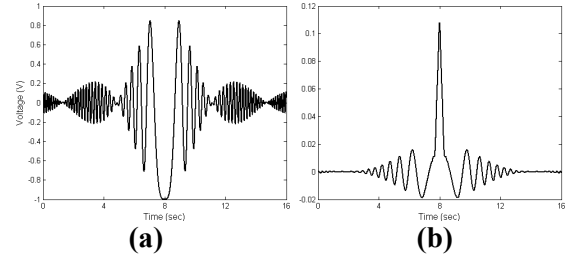


**Fig.10: a) Signal at the matched filter input, b) Signal at the correlator output.**

Figure 11 shows the signals of a scenario representing two humans on foot, separated by 1m. In Fig.11(a), the Tx/Rx separation is 30m, whereas in Fig.11(b) it is 100m. It is evident that irrespective of separation, the positions of the two targets can be identified with the same accuracy.

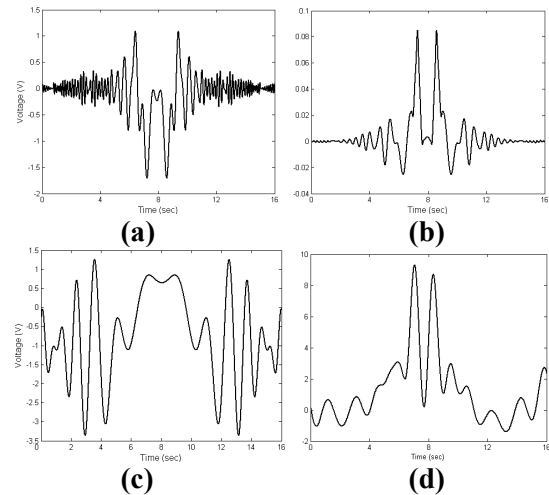


**Fig.11: Signal from two humans for: a) 30m Tx/Rx separation, b) Output for (a), c) 100m Tx/Rx separation, d) Output for (c).**

### *Small/Large Targets Resolution*

In order to detect a small target hidden within the background of the larger target's signature, we can take advantage of the fact that when a target crosses the baseline the Doppler frequency goes to zero. To measure the level of DC and the very low frequency level of the FT, a windowed FT is used, proceeding along the signal at fixed intervals. Fig.12 shows the plot of the received signal with the corresponding DC level, for a window length of 2 seconds; for when firstly only a tank is present, and then when a tank is followed by a human at a separation of 1m.

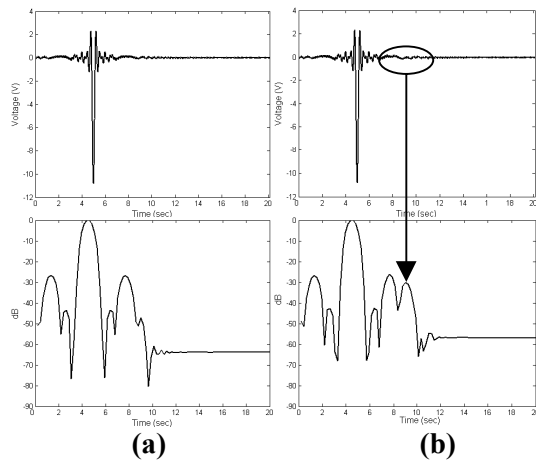


**Fig.12: The detection algorithm: a) Tank only b) Tank followed by a human at 1m.**

When a human follows the tank, the time domain signal clearly shows the tank signature but does not provide any insight as to the human signature. However, applying the DC level search algorithm yields an additional peak that indicates the

## REFERENCES

- 1 R.S.A. Raja Abdullah, M. Cherniakov "Forward Scattering Radar For Vehicles Classification", VehCom Int'l Conf., VehCom2003, 2003, pp.73-78.
- 2 R.S.A. Raja Abdullah, M. Cherniakov, P. Jančovič "Automatic Vehicle Classification In Forward Scattering Radar", 1st Int'l Workshop in Intelligent Transportation, WIT2004, Germany, 2004, pp.7-12.
- 3 R.S.A. Raja Abdullah, M. Cherniakov, P. Jančovič and M. Salous," Progress on Using Principle Component Analysis in FSR for Vehicle Classification", 2nd Int'l Workshop in Intelligent Transportation, WIT2005, Germany, 2005, pp. 7-12.
- 4 M. Cherniakov, R.S.A. Raja Abdullah, P. Jančovič and M. Salous," Forward Scattering Micro Sensor for Vehicle Classification ", To be presented at IEEE Int'l Radar Conf., Arlington, Virginia, USA, May 9-12, 2005.
- 5 M. Cherniakov, V. Chapursky, R.S.A. Raja Abdullah, P. Jančovič and M. Salous," Short-Range Forward

presence of the human. This simple method will be further refined during the next phase of work.

## Conclusions

Building on results, which clearly illustrate the classification capabilities of FSR, this paper presents work on characterising FSR. The system power budget, operating in line of sight (LOS) conditions, was evaluated at both theoretical and experimental level. We have demonstrated that an excellent resolution is achievable; the potential resolution of the system is equal to a target's horizontal dimension. The dynamic range of the system is also shown to be very high. Finally we have presented a simple algorithm for the detection of a small target whose signal is buried within the signal of a bigger target.

Scattering Radar", Int'l Conf. on Radar Sys. RADAR 2004, Toulouse, France.

- 6 V. Chapursky and V. Sablin," SISAR: Shadow Inverse Synthetic Aperture Radiolocation," Int'l Conf. on Radar Systems RADAR 2000, pp. 322-328.
- 7 T. Rappaport, Wireless Communications: Principles and Practice, Prentice-Hall, 1996, ISBN 0-13-375536-3.

## ACKNOWLEDGEMENTS

The work reported in this paper was funded by the Electro-Magnetic Remote Sensing (EMRS) Defence Technology Centre, established by the UK Ministry of Defence and run by a consortium of SELEX Sensors and Airborne Systems, Thales Defence, Roke Manor Research and Filtronic.